

NON-RANDOM DISTRIBUTION OF ADSORBATES ON CATALYTIC SURFACES: THE ROLE OF INTERACTIONS BETWEEN ADSORBATES

KESAVA RAO KAZA[†] and SANKARAN SUNDARESAN[‡]

*Department of Chemical Engineering
Princeton University, Princeton, New Jersey 08544*

(Received September 21, 1983; in final form February 6, 1984)

It has been repeatedly stressed in the literature that the commonly invoked assumption of a random distribution of adsorbates on the catalyst surface is suspect under certain operating conditions. Nonrandom distribution of the adsorbates can occur as a result of interaction between adsorbates and/or their inadequate mobility. We have studied the effect of adsorbate interactions on the rates and stability of catalytic reactions, and the salient features are outlined with several examples. An analysis of the thermodynamic data concerning the oxidation of SO₂ on platinum is presented within the framework of the proposed model.

KEYWORDS Adsorbate interactions Sulfur dioxide oxidation on noble metals
Phase separation of adsorbates

1. INTRODUCTION

When modeling catalytic reactions on metal surfaces, an assumption of ideal adsorption of the chemical species on substrate lattice is often invoked. Under conditions of ideal adsorption, quantities such as heats of adsorption and reaction remain independent of coverage. There is ample evidence to indicate that in many systems ideal adsorption is a questionable assumption [e.g., see 1, 2]. Deviations from ideality could be induced, for example, by surface heterogeneity.³ Several studies have shown that deviations from ideality are observed even on well-defined surfaces indicating that causes other than surface heterogeneity may also be responsible.² It is now well-established that the adsorbed species (adatoms) interact with each other. A detailed discussion of the forces leading to adatom interactions can be found in recent reviews by Lagally¹ and Einstein.⁴ Lattice gas models incorporating the interactions between adatoms have been studied quite extensively [e.g., see 1, 2, 5]. Interactions between adsorbed species lead to (i) coverage dependence of the equilibrium constant for the adsorption-desorption process,⁵ (ii) complex variation of the sticking probability with coverage,² and (iii) coverage dependence of the rate constant for desorption.² For an exhaustive survey of experimental data on formation of ordered

[†] Present address: Department of Chemical Engineering, Indian Institute of Science, Bangalore, India 560012.

[‡] Author to whom all correspondence should be addressed.

structure as a result of adatom interactions, see the recent monograph by Somorjai.⁶ Accounting for the adatom interactions via coverage dependence of the sticking probability and desorption rate constant is routinely practised now [e.g., see 2]. Judging from the extent of coverage dependence of sticking probabilities and desorption rate constants for several systems, it is quite conceivable that appreciable coverage dependence will be displayed by the surface reaction rate constants as well. Yet very little work has been done to understand the effects of adatom interactions on rates of chemical reactions taking place on metal surfaces.

One can cite several systems where adatom interactions are known to influence the surface rate processes appreciably—e.g., reduction of NO by CO on Pt,¹⁴ decomposition of species such as formic acid and nitromethane on Ni,¹⁰ and virtually every oxidation reaction on noble metal surfaces. Some recent results reported by Vayenas and Saltsburg⁷ indicate that during SO₂ oxidation on noble metal surfaces, formation of a condensed SO₃ phase may occur on the catalyst surface under certain operating conditions. The formation of such a condensed phase is thought to be caused by attractive interaction between adsorbed SO₃ molecules.

It has been repeatedly suggested that interactions between adsorbed species may, at least in part, be responsible for some of the complex reaction dynamics such as autonomous reaction rate oscillations.^{8,9} Wicke *et al.*¹¹ have emphasized the importance of non-random distribution of the adsorbed species on the catalyst surface in any effort to provide a meaningful explanation of autonomous reaction rate oscillation during CO oxidation. Non-random distribution of adsorbates can occur as a result of interaction between adsorbed species and/or inadequate mobility of the adsorbed molecules on the catalyst surface. In this paper we confine our attention to contributions of interactions between adsorbates and leave it to a future study to address the issue of finite mobility.

Pikios and Luss¹² studied a simple example where the activation energy for the bimolecular surface reaction is influenced by coverage of one of the species and showed that reaction rate oscillations could arise as a result of such an effect. However, Wicke *et al.*¹¹ stress that the effect of interactions on the rates of desorption process is probably the most important contribution. In this paper we present a scheme to account for the influence of adsorbate interactions on the rates of desorption and reaction, as well as the thermodynamics of the adsorbates. We shall first illustrate the model formulation with a unimolecular decomposition reaction. Then we shall extend the concepts introduced in this paper and present a plausible explanation for the thermodynamic data on SO₂ oxidation reported by Vayenas and Saltsburg.⁷ Finally, we shall reexamine the problem treated by Pikios and Luss¹² and analyse the role of adsorbate interactions as predicted by the proposed model.

2. MODEL FORMULATION

Our analysis is based on lattice gas models^{5,13,15–20} with the following assumptions.

1. The crystal surface can be modeled by a two-dimensional array of sites, such that each site has z nearest neighbors.
2. Each site can be occupied by at most one adatom.

3. Only nearest-neighbor interactions are considered.

4. The total interaction energy between an adatom and its nearest-neighbor occupied sites is the sum of pair interaction energies, the latter being treated as constants. Repulsive interactions are assigned positive values.

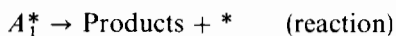
5. Following the quasi-chemical approach to lattice statistics, all pairs of sites are assumed to be independent.

6. Following Zhdanov,¹³ it is assumed that an activated complex does not interact with adatoms in the nearest neighbor sites. Further, the number of activated complexes is small compared to the number of adatoms.

7. The crystal (surface) is assumed to be under isothermal conditions. This restriction is quite critical in that it permits the assumption of adsorbate equilibrium over the surface.

Zhdanov¹³ has used absolute rate theory in conjunction with the above assumptions to derive expressions for the rates of adsorption, desorption and reaction. Here we extend his analysis to incorporate certain aspects of adsorbate thermodynamics. The exact solution for the lattice gas models can be obtained only for a limited number of cases. Hence different levels of approximations to the exact solutions have been proposed. The so-called quasi-chemical approximation^{5,13,15-20} is the simplest of these approximations that brings out the non-random nature of the adsorption caused by adsorbate interactions. However, this approximation requires specification of the number of nearest-neighbor sites for every adsorption site, z . When applying the results of this approximation to a polycrystalline catalyst surface, one encounters difficulties with specification of z . Fortunately, there exists the Bragg-Williams (or mean-field) approximation which circumvents this difficulty (as will be seen later). It is needless to say that this approximation is less accurate than the quasi-chemical approximation.⁵ Yet, it captures the essential features such as the role of interactions on the rates of desorption and reaction as well as adsorbate thermodynamics. Hence we present results only for the mean-field approximation. It must, however, be emphasized that the more accurate quasi-chemical model can be formulated quite readily,²¹ albeit at the expense of a greater algebraic exercise.

Let us consider the example of a unimolecular decomposition reaction on a catalyst surface.



where G_1 and A_1 denote gaseous and adsorbed species respectively and $*$ denotes an empty site. Let N_i and M denote the number of i -sites (sites occupied by adatoms of species i) and the total number of sites respectively. Henceforth, $i = 0$ will denote an empty site. In view of the assumptions discussed above, the rate of adsorption is proportional to

$$p_1(N_0/M) \equiv p_1\theta_0$$

where p_1 is the partial pressure of species 1. The above formalism therefore leads to a linear variation of the sticking probability with coverage. In practice, many systems

display very complex variation of sticking probability with coverage.²⁶ They can be accounted either by requiring a precursor state^{13,26} or by postulating nominal interactions between adsorbed molecules with the activated complexes.^{13,27} In the present work, for the sake of simplicity we shall be satisfied with the above description.

The rate of desorption is proportional to

$$\frac{N_1}{M} e^{m\epsilon_{11}/RT} \equiv \theta_1 e^{m\epsilon_{11}/RT}$$

where m is the average number of 1-neighbors of a 1-site and ϵ_{11} is the pair interaction energy between adatoms of species 1 (occupying adjacent sites). It can be shown that, within the framework of the mean-field model, $m = z\theta_1$ while the quasi-chemical approximation leads to a rather complex function.²¹ Thus the steady-state mass balance for species 1, in the mean-field model, takes the form

$$k_{d1}p_1\theta_0 - (k_{d1} + k_r)\theta_1 e^{\omega_{11}\theta_1} = 0 \quad (1)$$

where

$$\omega_{11} = \frac{z\epsilon_{11}}{RT}, \quad \theta_0 = 1 - \theta_1 \quad (2)$$

As seen from (1), desorption and reaction processes feel a similar effect as a result of the interactions.

The mathematical description of the problem is by no means complete. Equation (1) assumes that the adsorbates remain as a single homogeneous phase on the catalyst surface. It can be easily shown that for sufficiently large attractive interaction and over a certain range of pressures, Eq. (1) yields three solutions—two of which are stable while the third is metastable. The situation is analogous to the multiplicity problem encountered with (e.g. Van der Waal's) equation of state. To circumvent the multiplicity problem in an equation of state, one postulates that the fluid splits into a condensed phase (liquid) and a dilute phase (vapor) in mutual equilibrium, and this is quite consistent with the experimental evidence.

It is quite conceivable that a similar phase separation may occur in the adsorbate layer under consideration as well. Nucleation of a condensed phase may occur, for example, at defect sites on the crystal surface. If one accepts the postulate of phase separation if and when applicable, it can be shown⁵ that the adsorbates will separate into two phases, a dense phase and a dilute phase, over a range of surface compositions if

$$\omega_{11} < -4 \quad (3)$$

i.e., if there are sufficiently large attractive interactions ($\epsilon_{11} < 0$). When Eq. (3) holds, phase separation occurs if

$$\theta_{11} < \theta_1 < \theta_{12} \quad (4)$$

where θ_{11} and θ_{12} are the coverages of species 1 in the two phases, and θ_1 is the surface-averaged coverage. The coverages θ_{11} and θ_{12} are determined using the conditions of phase equilibrium between the two surface phases,⁵ namely, equality of chemical

potentials

$$\frac{\theta_{11}}{\theta_{01}} e^{\omega_{11}\theta_{11}} = \frac{\theta_{12}}{\theta_{02}} e^{\omega_{11}\theta_{12}} \tag{5}$$

and equality of spreading pressures

$$\frac{e^{\omega_{11}\theta_{11}^2/2}}{\theta_{01}} = \frac{e^{\omega_{11}\theta_{12}^2/2}}{\theta_{02}} \tag{6}$$

where

$$\theta_{0i} = 1 - \theta_{1i}, \quad i = 1,2. \tag{7}$$

It can be shown⁵ that solving Eqs. (5) and (6) is equivalent to finding the roots of

$$\frac{\theta_1}{1 - \theta_1} e^{\omega_{11}\theta_1} = e^{\omega_{11}/2}, \quad \theta_1 \neq 1/2 \tag{8}$$

and that

$$\theta_{11} + \theta_{12} = 1 \tag{9}$$

It can be argued that the above phase equilibrium conditions are applicable as long as the mobility of the adsorbates is very high, so that the tendency of the decomposition reaction to hold the surface at a non-equilibrium state is easily compensated by the mobilities. In a future study we shall address the issue of the non-equilibrium surface state caused by rapid reaction.

In the two-phase region Eq. (1) must be replaced by

$$k_{a1}p_1 \sum_{i=1}^2 f_i\theta_{0i} - (k_{d1} + k_r) \sum_{i=1}^2 f_i\theta_{1i}e^{\omega_{11}\theta_{1i}} = 0 \tag{10}$$

where f_i , the relative amount of phase i on the catalyst surface, is given by

$$\theta_1 = f_1\theta_{11} + f_2\theta_{12}; \quad f_1 + f_2 = 1 \tag{11}$$

Using Eqs. (8) and (11), Eq. (10) can be rewritten as

$$k_{a1}p_1\theta_0 - (k_{d1} + k_r)(1 - \theta_1)e^{\omega_{11}/2} = 0$$

or

$$\underline{p}_1 \equiv \frac{k_{a1}p_1}{(k_{d1} + k_r)e^{\omega_{11}/2}} = 1, \quad \theta_{11} < \theta_1 < \theta_{12}$$

Thus the two-phase region can occur at only one value of pressure, given by the above equation. At this pressure the surface-averaged coverage θ_1 can assume any value in the region $\theta_{11} < \theta_1 < \theta_{12}$ and the corresponding dimensionless reaction rate

$$\underline{r} \equiv \frac{\theta_1 e^{\omega_{11}\theta_1}}{e^{\omega_{11}/2}} = (1 - \theta_1), \quad \theta_{11} < \theta_1 < \theta_{12}$$

decreases as θ_1 increases. The phase transition is reflected by a discontinuity in the reaction rate, as shown in Figure 1. It is only fitting to re-emphasize the assumptions

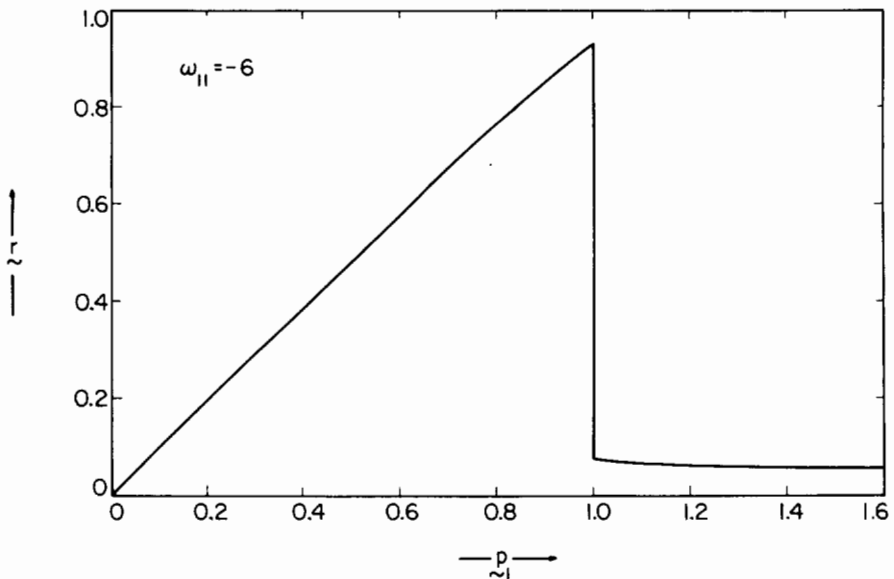


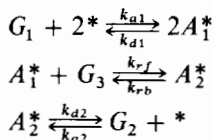
FIGURE 1 Dimensionless rate of decomposition reaction as a function of dimensionless partial pressure.

involved. The entire crystal surface is assumed to be under isothermal condition, thus allowing us to use arguments based on equilibrium thermodynamics, leading to results shown in Figure 1. However, if the adsorbates always remain as a single phase (i.e. Eq. (1) is valid under every condition), the discontinuity shown in Figure 1 does not obtain. Instead features such as isothermal multiplicity and hysteresis obtain. We shall not pursue this possibility as we are inclined to believe that the phase separation of the adsorbates is physically more reasonable. The "negative order" of the reaction rate for $p_1 > 1$ is due to the increased stability of the adsorbates as a result of attractive interactions. While in this simple reaction mechanism the two-phase region occurs at a unique gas phase condition, for more complex systems such as SO_2 oxidation (to be treated in the next section) the two-phase region will occur over a continuous range of conditions.

3. CONSEQUENCES OF ADSORBATE INTERACTIONS IN THE OXIDATION OF SULFUR DIOXIDE ON NOBLE METALS

The oxidation of sulfur dioxide on platinum has been studied for several decades and no attempt shall be made to review all these results. Instead, we simply refer to the recent work by Vayenas and Saltsburg⁷ and concern ourselves with an effort to model certain experimental observations by them. These authors used a high temperature solid electrolyte cell to monitor the oxygen activity on Pt, Au and Ag catalyst films exposed to mixtures of O_2 , SO_2 and SO_3 at temperatures above 400°C and atmospheric pressure. We are primarily concerned with the results on Pt surface. Under these experimental conditions oxygen adsorbs dissociatively on the surface.

Experimental evidence²²⁻²⁴ indicates that the concentration of adsorbed SO₂ at these elevated temperatures will be quite small and that under such oxidizing conditions very little S or SO will be present. These indicate that, for modeling purposes, SO₂ in the gas phase can be assumed to react with adsorbed oxygen directly to form adsorbed SO₃ which subsequently desorbs.⁷ Thus we have



where species $i = 1,2,3$ denote oxygen, SO₃ and SO₂, respectively. Here k_{ai} and k_{di} are the rate constants for the adsorption and desorption of species i respectively, while k_{rf} and k_{rb} are the rate constants for the forward and backward reaction respectively.

Within the framework of the above kinetic mechanism, we can summarize the oxygen activity data of Vayenas and Saltsburg⁷ as follows. There are three distinct regimes:

- (i) For $p_2 < K_2(T)K_3(T)$ and $p_3\sqrt{p_1} < K_2(T)$, we have $a_1 = \sqrt{p_1}$.
- (ii) For $p_2 < K_2(T)K_3(T)$ and $p_3\sqrt{p_1} > K_2(T)$, we have $a_1 < \sqrt{p_1}$ and $p_3a_1 = K_2(T)$.
- (iii) For $p_2 > K_2(T)K_3(T)$, $p_3\sqrt{p_1} > K_2(T)$ we have $a_1 < \sqrt{p_1}$ and $p_3a_1 = p_2/K_3(T)$.

Here $K_2(T)$ and $K_3(T)$ are experimentally measured functions of temperature whose physical interpretation in terms of the rate constants in the kinetic model will be discussed later.

It is quite straightforward to show that a model that assumes an ideal surface and random configuration for adsorbed species cannot explain these data.⁷ Here we show that the above data can be quite simply explained on the basis of interactions between adsorbed molecules.

A qualitative comparison with the properties of bulk condensed phase SO₃²⁵ led Vayenas and Saltsburg⁷ to speculate that a condensed SO₃ phase may be formed on the surface in regime (ii). Since the origin of such a condensed phase is quite possibly due to attractive interactions between adsorbed SO₃ molecules, we postulate such an interaction. Needless to say, repulsive interactions are more common in chemisorbed systems. However, attractive interactions cannot be ruled out. For example, Benziger and Schoofs¹⁰ provide convincing evidence for attractive interactions between adsorbed formates on nickel. Under experimental conditions encountered during the study of Vayenas and Saltsburg⁷ very little oxygen is present on the surface. The nonidealities in the adsorption of oxygen will therefore have a very small effect on the observed results. Hence we shall neglect interactions between adsorbed oxygen atoms as well as those between oxygen and SO₃. Furthermore, since we are dealing with high temperature reaction conditions, the mobilities of all the adsorbed species will indeed be quite high and hence the number of nearest-neighbor pairs (11, 12 and 22) can be expressed in terms of the coverages. Finally, as the experiments were conducted on polycrystalline Pt film and the temperatures were high, we present the mathematical results for the mean-field model only. In the context of the mean-field model, a precise

definition of the number of nearest-neighbor sites of any adsorption site is not needed, making such a model attractive for analysing data on polycrystalline film. (It must be emphasized that the following analysis was repeated using the more detailed quasi-chemical approximation. No qualitative differences were observed between the two models.)

When the adsorbed molecules exist as a single, homogeneous phase on the catalyst it can be shown that the steady-state species balances are given by

$$k_{a1}p_1\theta_0^2 - k_{d1}\theta_1^2 - k_{rf}p_3\theta_1 + k_{rb}\theta_2e^{\omega_{22}\theta_2} = 0 \quad (12)$$

$$k_{a2}p_2\theta_0 - (k_{d2} + k_{rb})\theta_2e^{\omega_{22}\theta_2} + k_{rf}p_3\theta_1 = 0 \quad (13)$$

where $\theta_0 = 1 - \theta_1 - \theta_2$ and ω_{22} is a parameter representing the interactions between adsorbed SO_3 molecules (< 0 for attractive). The other assumptions made in deriving Eqs. (12) and (13) are self-evident. Before proceeding further it is convenient to express θ_1 and θ_0 in terms of θ_2 and a'_1 , the partial pressure of gaseous oxygen that would be in equilibrium with the adsorbed oxygen. Assuming a perfect gas mixture, the chemical potential of the gaseous oxygen is given by

$$\mu'_1 = \mu'_{10}(T) + RT \ln a'_1$$

or

$$a'_1 = \lambda'_1/\lambda'_{10}$$

where $\lambda'_1 = \exp(\mu'_1/RT)$ is the absolute activity of gaseous oxygen. In view of the dissociative adsorption, the absolute activity of adsorbed oxygen is given by

$$\lambda_1 = \sqrt{\lambda'_1} = \sqrt{\lambda'_{10}a'_1} \quad (14)$$

Using equilibrium statistical thermodynamics,⁵ we get

$$\lambda_1 = \frac{1}{j_1(T)} \frac{\theta_1}{\theta_0} \quad (15)$$

where $j_1(T)$ is the partition function for an adsorbed oxygen atom. Defining

$$K_1(T) = j_1(T)\sqrt{\lambda'_{10}}, \quad a_1 = \sqrt{a'_1} \quad (16)$$

Eqs. (13) and (14) can be combined to give

$$\frac{\theta_1}{\theta_0} = K_1 a_1 \equiv c_1 \quad (17)$$

If the adsorbed oxygen atoms are in equilibrium with gaseous oxygen molecules at a partial pressure p_1 , Eqs. (12) and (16) imply that

$$\frac{\theta_1}{\theta_0} = \sqrt{k_{a1}/k_{d1}} \sqrt{p_1}, \quad a_1 = \sqrt{p_1}$$

or, by using (17),

$$K_1 = \sqrt{k_{a1}/k_{d1}} \quad (18)$$

This result will be useful later on. It can be further shown that

$$\theta_0 = \frac{1 - \theta_2}{1 + c_1}, \quad \theta_1 = \frac{(1 - \theta_2)c_1}{1 + c_1} \quad (19)$$

Thus Eqs. (12) and (13) can be rewritten as

$$\frac{k_{a1} p_1 g(\theta_2)}{(1 + c_1)^2} - \frac{k_{d1} g(\theta_2) c_1^2}{(1 + c_1)^2} - \frac{p_3 c_1}{1 + c_1} + k_{rb} h(\theta_2) = 0 \quad (20)$$

$$\frac{k_{a2} p_2}{1 + c_1} - (k_{d2} + k_{rb}) h(\theta_2) + \frac{p_3 c_1}{1 + c_1} = 0 \quad (21)$$

where

$$k_{ai} = k_{ai}/k_{rf}; \quad k_{di} = k_{di}/k_{rf} \quad (i = 1, 2)$$

$$k_{rb} = k_{rb}/k_{rf}$$

$$g(\theta_2) = 1 - \theta_2 \quad (22)$$

$$h(\theta_2) = \frac{\theta_2 e^{\omega_{22}\theta_2}}{1 - \theta_2}$$

Thermodynamic stability criteria⁵ suggest that the adatoms may divide into a dense phase and a dilute phase over a certain range of surface compositions if

$$\omega_{22} < -4 \quad (23)$$

The inherent polycrystalline nature of the Pt film on which experiments were conducted makes one suspect whether such a phase separation criterion is appropriate. To answer this, we examined the case where phase separation can occur as well as that where no such phase separation is permitted. It was found that a much better agreement between model predictions and the experimental data of Vayenas and Saltsburg⁷ obtains if phase separation of the adsorbates when required by thermodynamics is permitted. Sample comparisons of the two cases will be shown later.

If and when the adatoms undergo phase separation, it can be shown that no more than two phases will be present on the catalyst surface, within the framework of the model under discussion. The fractional coverages in the two coexisting phases are described by the following.

a) Equality of chemical potentials:

$$\frac{\theta_{11}}{\theta_{01}} = \frac{\theta_{12}}{\theta_{02}} \quad (24)$$

$$\frac{\theta_{21}}{\theta_{01}} e^{\omega_{22}\theta_{21}} = \frac{\theta_{22}}{\theta_{02}} e^{\omega_{22}\theta_{22}} \quad (25)$$

b) Equality of spreading pressures:

$$\frac{e^{\omega_{22}\theta_{21}^2/2}}{\theta_{01}} = \frac{e^{\omega_{22}\theta_{22}^2/2}}{\theta_{02}} \quad (26)$$

where θ_{ij} is the coverage of species i in phase j . The coverages θ_{ij} can be related to the surface-averaged coverages θ_i by

$$\sum_{j=1}^2 f_j \theta_{ij} = \theta_i \quad i = 1, 2 \quad (27)$$

$$\sum_{j=1}^2 f_j = 1$$

where f_j is the fraction of the catalyst surface covered by phase j . Equations (24)–(26) can be simplified to yield that θ_{21} and θ_{22} are the roots of

$$\frac{\theta_2}{1 - \theta_2} e^{\omega_{22}\theta_2} = e^{\omega_{22}/2} \quad \theta_2 \neq 1/2 \quad (28)$$

One can then proceed to solve Eqs. (24) and (27) to obtain f_j and θ_{1j} in terms of the surface-averaged coverages θ_1 and θ_2

$$f_1 = 1 - f_2 = \frac{\theta_{22} - \theta_2}{\theta_{22} - \theta_{21}} \quad (29)$$

$$\frac{\theta_{1i}}{\theta_1} = \frac{1 - \theta_{2i}}{1 - \theta_2} \quad i = 1, 2$$

When the adspecies exist in two phases, the species balance Eqs. (12) and (13) must be suitably modified to read

$$\sum_{j=1}^2 f_j [k_{a1} p_1 \theta_{0j}^2 - k_{d1} \theta_{1j}^2 - k_{rf} p_3 \theta_{1j} + k_{rb} \theta_{2j} e^{\omega_{22}\theta_{2j}}] = 0$$

$$\sum_{j=1}^2 f_j [k_{a2} p_2 \theta_{0j} - (k_{d2} + k_{rb}) \theta_{2j} e^{\omega_{22}\theta_{2j}} + k_{rf} p_3 \theta_{1j}] = 0$$

After combining these equations with Eq. (29), we recover Eqs. (20) and (21) for the two phase region as well, provided Eq. (22) is replaced by

$$g(\theta_2) = 1 - \frac{\theta_{21}\theta_{22}}{1 - \theta_2}; \quad h(\theta_2) = e^{\omega_{22}/2} \quad \text{for } \theta_{21} < \theta_2 < \theta_{22} \quad (30)$$

It will now be shown that the above model is consistent with the activity data of Vayenas and Saltsburg.⁷

Regimes (i) and (ii)

The inequality $p_2 < K_2 K_3$ can be satisfied by choosing p_2 sufficiently small. To simplify the analysis, we set $p_2 = 0$ in Eqs. (20) and (21). The resulting equations can be solved for c_1 and p_3 in terms of θ_2 to get

$$c_1 = \frac{-\underline{k}_{d2} h + \sqrt{\Delta_0}}{\underline{k}_{d2} h + \underline{k}_{d1} g} \quad (31)$$

where

$$\Delta_0 = \underline{k}_{d2}^2 h^2 + [\underline{k}_{d1} g + \underline{k}_{d2} h][\underline{k}_{a1} p_1 g - \underline{k}_{d2} h]$$

and

$$\frac{p_3 c_1}{1 + c_1} = (k_{d2} + k_{rb})h \tag{32}$$

The functions g and h are defined by Eqs. (22) and (30) in the single and two phase regions respectively.

If we now consider the limit $\theta_2 \rightarrow 0$ (i.e. very little SO_3 on the surface),

$$h \rightarrow 0, \quad g \rightarrow 1, \quad c_1 \rightarrow K_1 \sqrt{p_1} \quad (\text{from Eq. (40)})$$

and

$$p_3 \rightarrow 0 \quad (\text{i.e. } p_3 \sqrt{p_1} \text{ will be less than } K_2)$$

Since $c_1 = K_1 a_1$, we can write

$$\lim_{p_3 \rightarrow 0} a_1 = \sqrt{p_1}$$

consistent with experimental observation in regime (i). It must be remarked that the activity data in regime (i) will be satisfied by literally any model with arbitrary set of assumptions. Hence, concordance between experimental data and prediction in regime (i) cannot be used to substantiate any given model.

Let us now consider the effect of increasing SO_2 partial pressure (p_3) while keeping p_1 fixed and $p_2 < K_2 K_3$. The immediate effect will be an increase in the surface coverage of $\text{SO}_3(\theta_2)$. Now in the limit, $\theta_2 \rightarrow \theta_2^*$ where θ_2^* is given by

$$k_{a1} p_1 g(\theta_2^*) - k_{d2} h(\theta_2^*) = 0$$

one obtains from Eqs. (31) and (32) that

$$c_1 \rightarrow 0$$

$$p_3 c_1 \rightarrow (k_{d2} + k_{rb})h(\theta_2^*)$$

While the exact value of θ_2^* is not obvious, if we insist that $\theta_{21} \leq \theta_2^* \leq \theta_{22}$ (i.e. surface composition is in the potentially two-phase region) and that the adlayer will separate into two phases as dictated by thermodynamics, it follows from Eq. (30) that

$$p_3 c_1 \rightarrow (k_{d2} + k_{rb})e^{\omega_{22}/2} = \text{constant}$$

Since $c_1 = K_1 a_1$, we obtain

$$p_3 a_1 \rightarrow \frac{(k_{d2} + k_{rb})e^{\omega_{22}/2}}{K_1} \equiv K_2(T) \tag{33}$$

while p_1 remains constant, $a_1 \rightarrow 0$ and hence we have $a_1 < \sqrt{p_1}$ and $p_3 \sqrt{p_1} > K_2(T)$. This behavior is consistent with regime (ii) and Eq. (33) relates the experimentally measured $K_2(T)$ in terms of model parameters. For both platinum and silver films, it was observed⁷ that $p_3 a_1 = K_2(T)$ whereas for a gold film

$$p_3 a_1 = K_2(T)(1 + K_4(T)a_1)$$

The former behavior is predicted asymptotically by the proposed model while the latter is predicted exactly by Eq. (32) in the two-phase region. Thus, within the framework of

the model, regime (ii) can be identified as one where two adphases are in coexistence on the catalyst surface.

Regimes (ii) and (iii)

Here we are concerned with the effect of increasing SO_3 partial pressure in the gas phase. We assume that p_1 and p_3 are kept fixed, such that $p_3\sqrt{p_1} > K_2(T)$. Equations (20) and (21) can then be solved for c_1 and p_2 in terms of θ_2 to obtain

$$c_1 = \frac{(2k_{rb}h - p_3) \pm \sqrt{\Delta_1}}{2\Delta_2} \quad (34)$$

$$k_{a2}p_2 = (k_{d2} + k_{rb})h(1 + c_1) - p_3c_1 \quad (35)$$

where

$$\begin{aligned} \Delta_1 &= (2k_{rb}h - p_3)^2 + 4\Delta_2(k_{a1}p_1g + k_{rb}h) \\ \Delta_2 &= p_3 + k_{d1}g - k_{rb}h \end{aligned} \quad (36)$$

Physically acceptable values of c_1 ($c_1 \geq 0$) are obtained only when $\Delta_2 \geq 0$ and the positive root is used in Eq. (34). As $\theta_2 \rightarrow 0$, $g \rightarrow 1$, $h \rightarrow 0$ and hence $\Delta_2 > 0$. However, as $\theta_2 \rightarrow 1$, $g \rightarrow 0$, $h \rightarrow \infty$ and hence $\Delta_2 < 0$. With the postulate of phase separation, the equation $\Delta_2 = 0$ has a unique root $\theta_2 = \theta'_2$. In the limit $\theta_2 \rightarrow \theta'_2$, Eqs. (34)–(36) imply that

$$\frac{p_3a_1}{p_2} \rightarrow \frac{[k_{rb}h(\theta'_2) - k_{d1}g(\theta'_2)]k_{a2}}{K_1[k_{d2}h(\theta'_2) + k_{d1}g(\theta'_2)]}$$

If the parameter values are such that θ'_2 is close to unity, then $h(\theta'_2) \gg g(\theta'_2)$ and hence the above equation reduces to

$$\frac{p_3a_1}{p_2} \rightarrow \frac{k_{a2}k_{rb}}{k_{d2}K_1} \equiv \frac{1}{K_3(T)} \quad (37)$$

As shown later, the above asymptote can be obtained even for $a_1 < \sqrt{p_1}$ provided suitable values for the model parameters are used. Equation (37) is experimentally observed in regime (iii) and we thus have an interpretation of $K_3(T)$ in terms of model parameters. Recalling that the above asymptote is obtained as $\theta_2 \rightarrow \theta'_2$, we conclude that the regime (iii) is obtained for sufficiently large values of p_2 . Experimental results also provide a lower bound for p_2 ($= K_2(T)K_3(T)$) below which regime (iii) is not realized. We can use this bound to derive some restrictions on the range of values for model parameters.

If we postulate that

$$k_{rb}h(\theta_2), k_{d1}g(\theta_2) \ll p_3 \quad (38)$$

it then follows from Eq. (34) that

$$p_3a_1 \simeq \frac{k_{a1}p_1g + k_{rb}h}{K_1} \quad (39)$$

Noting that h is a constant and g is bounded in the two phase region, p_3a_1 will vary

slowly with θ_2 if

$$k_{rb}h \gg \underline{k}_{a1}p_1g \quad \text{for} \quad \theta_{21} < \theta_2 < \theta_{22} \quad (40)$$

When (38)–(40) are introduced in Eq. (21), we get

$$\underline{k}_{a2}p_2 \simeq \underline{k}_{d2}h - \underline{k}_{a1}p_1g \quad (41)$$

If the parameter values are such that the two terms on the rhs of Eq. (41) are comparable in the two phase region, p_2 varies more rapidly with θ_2 than does p_3a_1 (Eq. (39)) and hence the inequality (40) may be replaced by

$$k_{rb} \gg \underline{k}_{d2} \quad (42)$$

This is consistent with the arguments of Vayenas and Saltsburg.⁷

On the basis of the arguments above, we can summarize the model predictions as follows. At very small values of p_2 and p_3 [defined by $p_3\sqrt{p_1} < K_2(T)$ and $p_2 < K_2(T)K_3(T)$], the surface coverage of SO_3 , θ_2 is quite small. In fact, $\theta_2 < \theta_{21}$ and regime (i) obtains. Now, as p_3 is increased so that $p_3\sqrt{p_1} > K_2(T)$ while maintaining $p_2 < K_2K_3$, θ_2 increases beyond θ_{21} and the adlayer separates into two phases. Furthermore θ_2 remains smaller than θ_{22} . Now if one increases p_2 so that $p_2 > K_2K_3$ while maintaining $p_3\sqrt{p_1} > K_2$, θ_2 increases beyond θ_{22} . There will then be only a single, but dense phase on the surface. In other words, the three regimes observed experimentally are simply described in terms of the proposed model as follows.

- regime (i) $\theta_2 < \theta_{21}$
- regime (ii) $\theta_{21} < \theta_2 < \theta_{22}$
- regime (iii) $\theta_2 > \theta_{22}$

4. SAMPLE CALCULATIONS

At 866 K, the experimental value of K_2 is approximately equal to $1.0 \text{ (kPa)}^{1.5}$ and this value will be used in the calculations discussed below. Using the inequalities derived earlier as guidelines, the following parameter values are chosen (at $T = 866 \text{ K}$)

$$\begin{aligned} \omega_{22} &= -6, & p_1 &= 20 \text{ kPa}, & K_1 &= 10^{-2} \text{ (kPa)}^{-0.5} \\ \underline{k}_{a1} &= 1.5 \times 10^{-4}, & \underline{k}_{d1} &= \underline{k}_{a1}/K_1^2 = 1.5 \text{ kPa} \\ (\underline{k}_{d2} + \underline{k}_{rb})e^{\omega_{22}/2} &= K_1K_2 = 0.01 \text{ (kPa)} \\ \underline{k}_{d2} &= 0.1 \underline{k}_{rb} \end{aligned}$$

With this choice of ω_{22} , one obtains from Eq. (28) that

$$\theta_{21} = 0.0707 \quad \text{and} \quad \theta_{22} = 0.9293$$

Case I: $p_2 = 0$

Figure 2 shows a plot of p_3a_1 vs. p_3 . The full curve corresponds to the phase separation model, while the broken curve represents results obtained by using the single phase equations throughout. Both cases yield the desired asymptotic behavior,

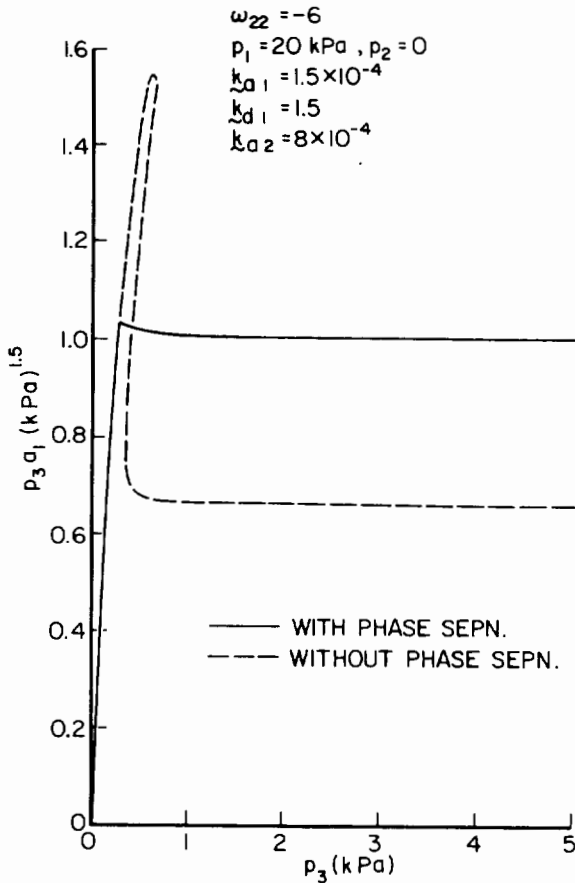


FIGURE 2 Effect of SO_2 partial pressure (p_3) on $p_3 a_1$.

namely, $p_3 a_1 \rightarrow \text{constant}$ for large values of p_3 . However, one difference should be noted. The experimental observations imply that this must be true for $p_3 > K_2/\sqrt{p_1} \equiv p_3^*$. The values of p_3^* for the two models are 0.22 kPa and 0.15 kPa, respectively. As seen in Figure 2, the variation of $p_3 a_1$ in the region $p_3 > p_3^*$ is much smaller for the two-phase model than for the single phase model. The quantity $a_1/\sqrt{p_1}$ is plotted against p_3 in Figure 3. For $p_3 < p_3^*$, $a_1/\sqrt{p_1}$ varies by about 16% and this is in reasonable agreement with activity data in regime (i). While $a_1/\sqrt{p_1}$ decreases smoothly as p_3 increases in the case of two-phase model, the single phase model implies a discontinuous change in $a_1/\sqrt{p_1}$ when p_3 takes on a critical value. Unfortunately, this is outside the range of p_3 values used in the experiments.⁷ Hence, discrimination between the two models is hardly justified in this context.

Case 2: $p_2 \geq 0, p_3 = \text{constant}$

Figure 4 shows a plot of $p_3 a_1$ against p_2 for $p_1 = 20$ kPa and $p_3 = 2$ kPa. For large values of p_3 , the curve asymptotes the line $p_3 a_1 = p_2/K_3(T)$ with $K_3 = 1.4 (\text{kPa})^{-0.5}$.

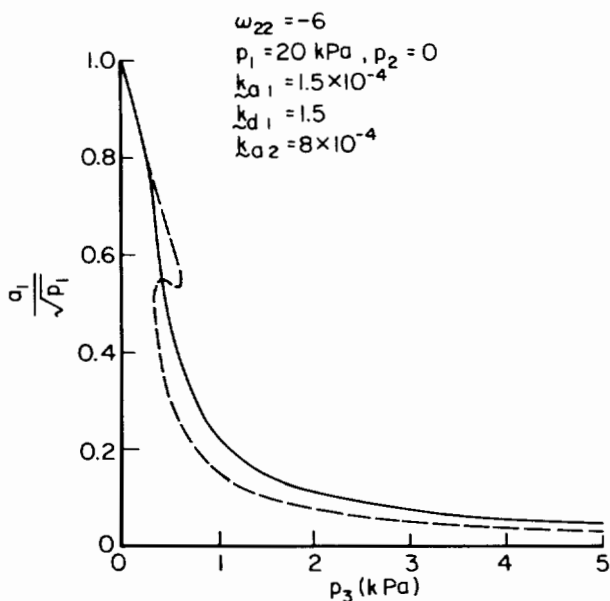


FIGURE 3 Effect of SO_2 partial pressure on the activity ratio ($a_1/\sqrt{p_1}$) for oxygen.

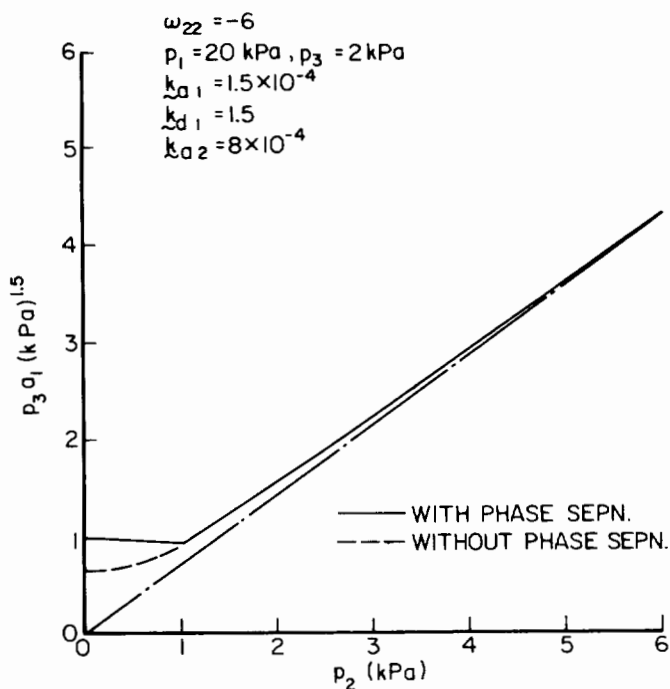


FIGURE 4 Effect of SO_3 partial pressure (p_2) on $p_3 a_1$.

Activity data⁷ imply that this should occur for $p_2 > K_2 K_3 \equiv p_2^* = 1.4$ kPa. With the present parameter values, the ratio $p_2/(p_3 a_1)$, increases from 1.22 to 1.4 as p_2 increases beyond p_2^* . In the region $0 \leq p_2 \leq p_2^*$, the quantity $p_3 a_1$ varies by about 20% for the two-phase model, while corresponding variation for the single phase model is about 70%. Thus the postulation of phase separation reduces the discrepancy between theory and experiment. Further, the slope of the experimental $p_3 a_1$ vs. p_2 curve appears to change abruptly at $p_2 = p_2^*$. This is qualitatively similar to the predictions of the two-phase model. On the other hand, the single phase model predicts a continuous variation of the slope.

Finally, Figure 5 shows that the results of the two-phase model for two different values of p_3 are virtually indistinguishable. Thus the slope $1/K_3$ is indeed independent of p_3 , in excellent agreement with the experimental results. We note in passing that the present value of K_3 ($= 1.4 \text{ kpa}^{-0.5}$) is of the same order as the measured value for $T = 866 \text{ K}$ ($= 1.1 \text{ kpa}^{-0.5}$).

To emphasize the importance of taking into account the adsorbate interactions, the results obtained for the case of no interactions (i.e., $\omega_{22} = 0$) are shown in Figures 6 and 7. Comparing these with Figures 2 and 4, we conclude the discrepancy between theory and experiment is much greater if the interactions are neglected.

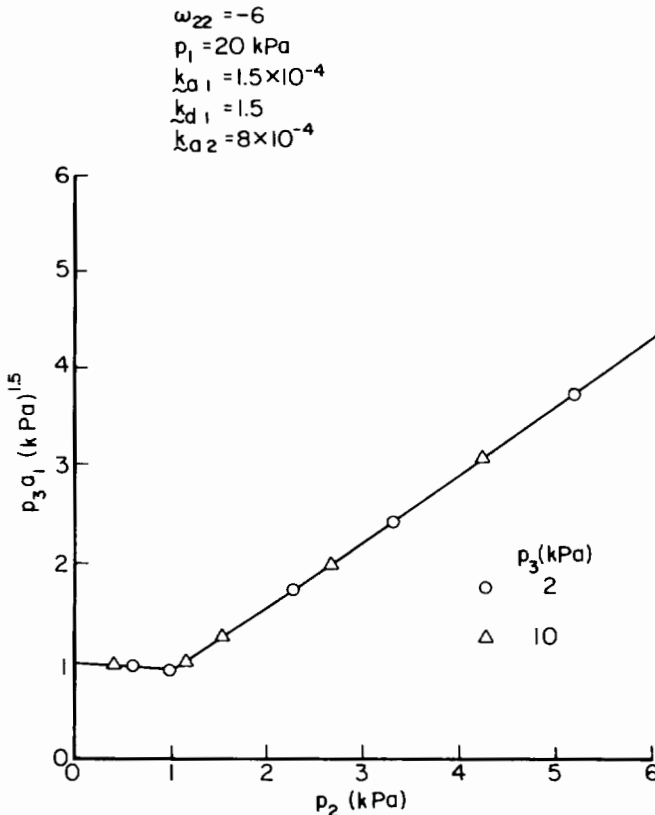


FIGURE 5 Effect of SO_3 partial pressure on $p_3 a_1$ at different SO_2 partial pressures.

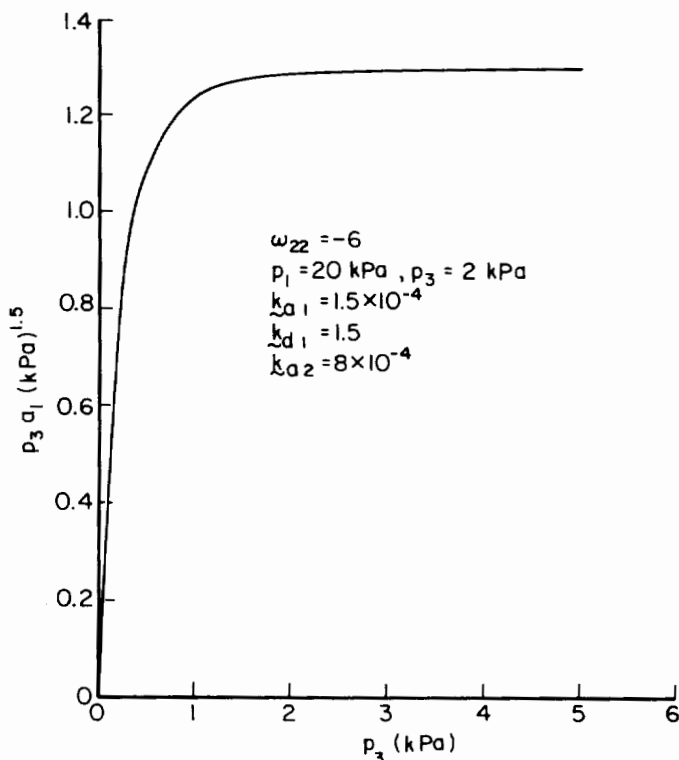


FIGURE 6 Effect of SO₂ partial pressure (p_3) on $p_3 a_1$. The case of no interactions, i.e., $\omega_{22} = 0$.

In conclusion, it has been shown that the postulates of attractive interactions and phase separation lead to results which are in good agreement with the results of Vayenas and Saltsburg.⁷ The model parameters were chosen in an ad hoc manner and it remains to be seen if their values can be substantiated with independent experiments. We also note that the models were developed for a single crystal surface, whereas a polycrystalline film was used by Vayenas and Saltsburg. The single plane results can be expected to carry over to the polycrystalline case only if one type of plane predominates, or alternatively, the reaction is structure-insensitive.

5. ISOTHERMAL REACTION RATE OSCILLATIONS

Many reactions on metal surfaces have been observed to exhibit oscillatory behavior for certain ranges of parameters.^{8,9,11} Several models have been proposed, each emphasizing a particular factor thought to be responsible for the observed rate oscillations. We shall not attempt to summarize the state-of-the-art modeling of the oscillations. Several excellent sources available in the literature provide such a summary.^{8,9,11,28-30} In this study we confine our attention to the role of interactions

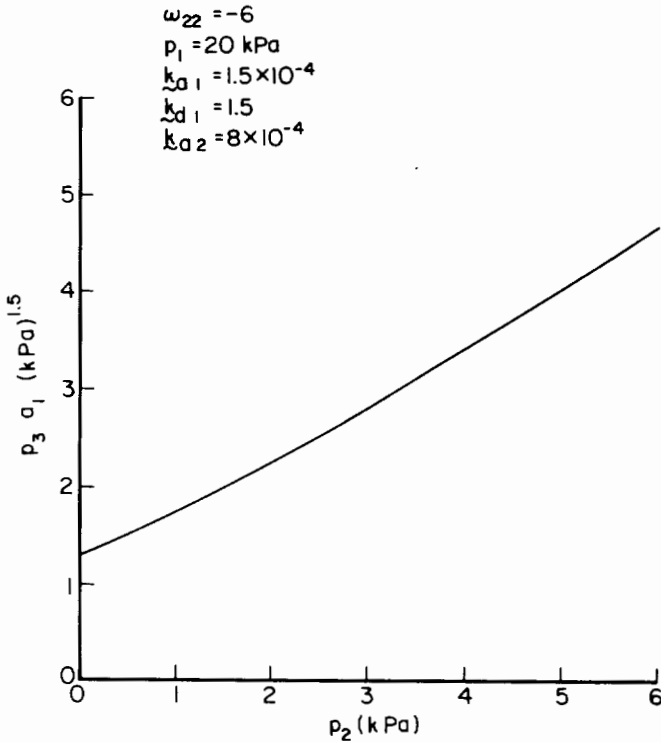
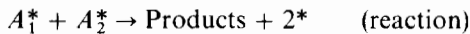
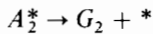
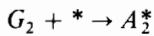


FIGURE 7 Effect of SO_3 partial pressure (p_2) on $p_3 a_1$. The case of no interactions, i.e., $\omega_{22} = 0$.

between adsorbates. The model system is the same as that studied by Pikios and Luss.¹²



To keep the analysis simple we assume that the pair interaction energies ϵ_{11} and ϵ_{12} are zero. Then it can be shown that the mean field equations take the form

$$\frac{d\theta_1}{d\tau} = k_{a1} p_1 \theta_0 - k_{d1} \theta_1 - \theta_1 \theta_2 e^{\omega_{22} \theta_2} \quad (43)$$

$$\frac{d\theta_2}{d\tau} = k_{a2} p_2 \theta_0 - k_{d2} \theta_2 e^{\omega_{22} \theta_2} - \theta_1 \theta_2 e^{\omega_{22} \theta_2} \quad (44)$$

where

$$\tau = t/k_r, \quad \omega_{22} = \frac{z\epsilon_{22}}{RT}, \quad \omega'_{22} = \frac{(z-1)\epsilon_{22}}{RT}$$

$$\underline{k}_{ai} = k_{ai}/k_r, \quad \underline{k}_{di} = \frac{k_{di}}{k_r}, \quad i = 1, 2$$

and k_r is the rate constant for the Langmuir-Hinshelwood reaction. It is interesting to note that in contrast to the model used by Pikios and Luss¹² the present model displays the effect of interactions on the reaction as well as the desorption processes. In fact, the interactions have a slightly greater effect on the desorption rate than on the reaction rate—much like the scenario suggested by Wicke.¹¹ Since z values are in the range of 4 to 6, it is reasonable to approximate ω'_{22} by ω_{22} . This has the virtue of making the functional dependence on θ_2 identical for both the desorption and reaction terms.

As discussed in the earlier examples, Eqs. (43) and (44) are valid only if the adsorbates remain on the surface as a single, homogeneous phase. It can be shown that if $\omega_{22} < -4$, the thermodynamic stability criterion predicts a separation of the adsorbates into two phases. The results of our study of the SO₂ oxidation problem (discussed earlier) suggest that it is reasonable to require such a phase separation and therefore we shall incorporate this phase separation in this example as well. Equations (43) and (44) above should be suitably modified in the two-phase region. The procedure for this modification is identical to that discussed in the previous two examples and hence the details will not be repeated here.

A careful study of the model equations were undertaken to elucidate its stability characteristics.²¹ It was found that oscillatory solutions can result for certain parameter values. This is shown in Figure 8 where surface averaged coverages θ_1 and θ_2 are shown in a phase plane. The parameter values used are:

$$\omega_{22} = -6, \quad \underline{k}_{a1}p_1 = 7 \times 10^{-3}, \quad \underline{k}_{d1} = 5 \times 10^{-4},$$

$$\underline{k}_{a2}p_2 = 8 \times 10^{-3}, \quad \text{and} \quad \underline{k}_{d2} = 1.488 \times 10^{-2}.$$

In this case the equations admit a unique steady-state, which is indicated by the symbol * in Figure 8. The two-phase region (on the basis of thermodynamics) corresponds to $0.0707 < \theta_2 < 0.9293$. Thus, if the surface-averaged coverages θ_1 and θ_2 are such that $0.0707 < \theta_2 < 0.9293$, the adsorbates exist on the surface as two phases. Note that the steady state (Figure 8) lies in the two-phase region. It can be easily shown that this steady-state is unstable and that a stable limit cycle obtains. This limit cycle along with a few sample trajectories are shown in Figure 8. It is easy to see from this figure that the adsorbate layer exists as two phases most of the time and the size of (i.e., the fraction of the surface occupied by) the condensed phase changes in time in a periodic fashion. It is very tempting to compare this with the picture envisioned by Wicke¹¹ for the oscillation cycle (i.e. the periodic growth and destruction of adsorbate clusters). While a very large value of the interaction energy was required to induce oscillations in the study of Pikios and Luss,¹² the present study shows that, when properly accounted for, modest levels of non-ideality suffice to induce oscillations.

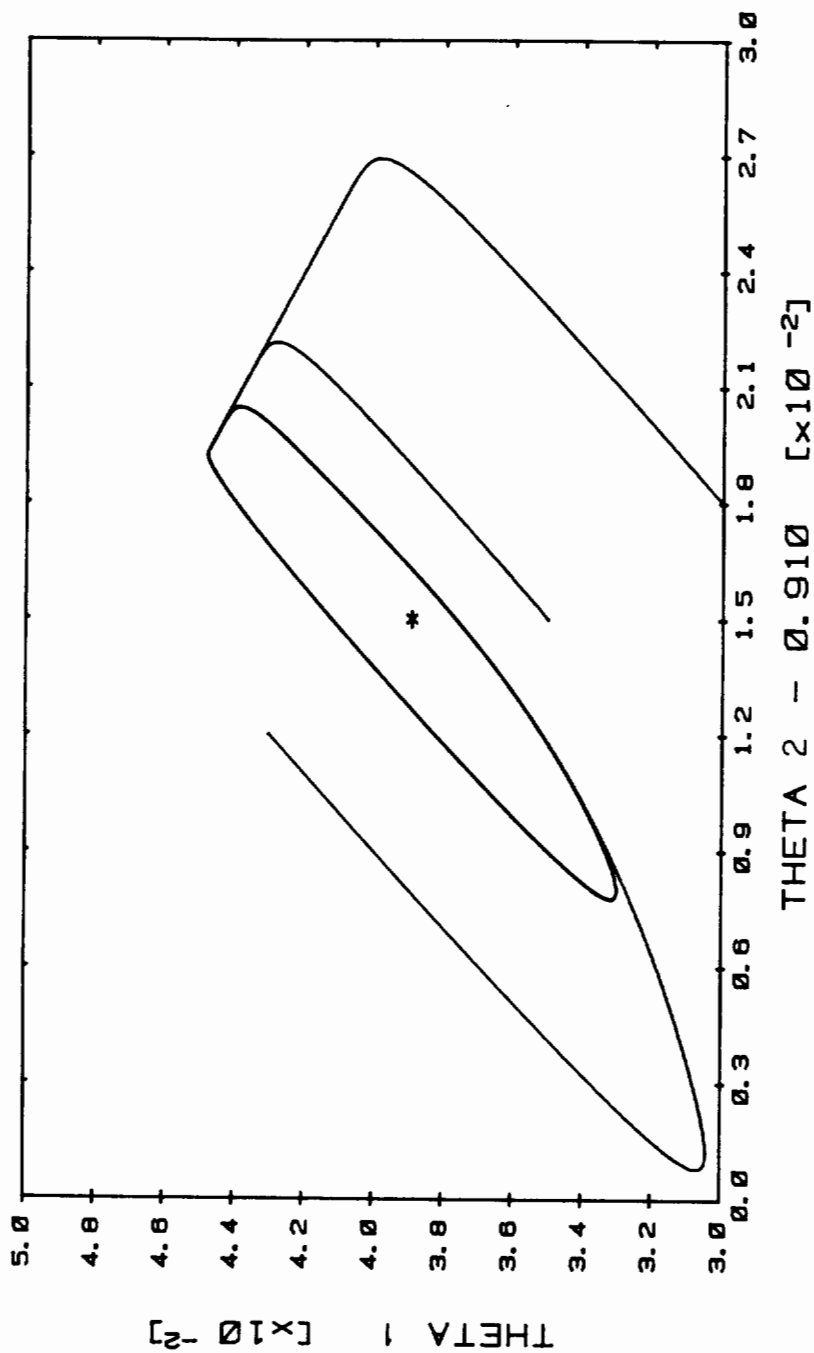


FIGURE 8 The phase plane for a case with unique, unstable steady state.

6. SUMMARY

The work was inspired by Wicke *et al.*'s¹¹ observation that non-random distribution of the adsorbed species on the catalyst surface may have a significant role in an ultimate explanation of complex pathological behavior such as rate oscillations and that the ability to model the non-randomness in a systematic, yet simple, way is lacking. Non-random distribution of the adsorbates can occur as a result of interactions between adsorbates and/or inadequate mobility of the adsorbates. In this paper the effect of interactions between adsorbates on the rates and stability of catalytic reactions have been studied and the salient features are outlined with three examples. The role of inadequate mobility may lead to even more intriguing results, and these will be addressed in a future publication.

ACKNOWLEDGMENTS

Acknowledgment is made to the donors of the Petroleum Research Fund, administered by the ACS (PRF # 13482-AC5), The Camille and Henry Dreyfus Foundation, Inc. (SG-31-81), the Atlantic Richfield Foundation, and the Shell Foundation for support of this work.

NOMENCLATURE

a_1	activity of adsorbed oxygen atoms
A_i	notation used to represent species i in the adsorbed layer
c_1	constant defined by Eq. (17)
f_i	fraction of catalyst surface covered by phase i
g	see Eqs. (22) and (30)
G_i	notation used to represent species i in the gas phase
h	see Eqs. (22) and (30)
k_{ai}	rate constant for adsorption of species i
k_{di}	rate constant for desorption of species i
k_r	rate constant for L-H reaction
k_{rf}	rate constant for forward reaction
k_{rb}	rate constant for reverse reaction
K_1	equilibrium constant for oxygen adsorption
K_2, K_3, K_4	experimentally determined quantities—functions of temperature only
M	total number of surface sites
N_i	number of surface sites occupied by species i ($i = 0$ denoting unoccupied sites)

p_i	partial pressure of species i in the gas phase
R	gas constant
t	time
T	temperature
z	number of nearest-neighbor sites

Greek Symbols

θ_0	fraction of unoccupied sites
θ_i	fraction of surface occupied by species i
θ_{ij}	fraction of surface in phase j occupied by species i
ϵ_{ij}	interaction energy between ij pair (i.e., species i and j occupying adjacent sites)
ω_{ij}	dimensionless interaction energy between ij pair
τ	dimensionless time

Subscripts

0	unoccupied site
i	species index
\sim	normalized variable

REFERENCES

1. Lagally, M.B., *et al.*, *CRC Critical Reviews in Solid State and Material Sciences*, **7**(3), 233 (1973).
2. King, D.A., *ibid.*, **7**(3), 167 (1978).
3. Laidler, K.J., in *Catalysis I*, P. Emmett, Ed., Reinhold Pub., NY, pp. 75–243 (1956).
4. Einstein, T.L., *CRC Critical Review in Solid State and Materials Sciences*, **7**(3), 261 (1978).
5. Fowler, R., and Guggenheim, E.A., in *Statistical Thermodynamics*, University Press, Cambridge, pp. 426–446 (1956).
6. Somorjai, G.A., in *Chemistry in Two Dimensions: Surfaces*, Cornell University Press, pp. 176–282 (1981).
7. Vayenas, C.G., and Saltsburg, H.M., *J. Catal.*, **57**, 206 (1979).
8. Slin'ko, M.G., and Slin'ko, M.M., *Cat. Rev. Sci. & Eng.*, **17**(1), 119 (1978).
9. Sheintuch, M., and Schmitz, R.A., *ibid.*, **15**(1), 107 (1977).
10. Benziger, J.B., and Schoofs, G.R., submitted to *J. Phys. Chem.* (1983).
11. Wicke, E., Kummann, P., Keil, W., and Schiefler, J., *Ber. Bunsenger. Phys. Chem.*, **84**, 315 (1980).
12. Pikios, C.A., and Luss, D., *Chem. Eng. Sci.*, **32**, 191 (1977).
13. Zhdanov, V.P., *Surface Science*, **102**, L35 (1981); **111**, L662 (1981); **111**, 63 (1981).
14. Gorte, R.J., and Schmidt, L.D., *Surface Science*, **111**, 260 (1981).
15. Hill, T.L., *An Introduction to Statistical Thermodynamics*, Addison-Wesley, Reading (1960).
16. Peierls, R., *Proc. Camb. Phil. Soc.*, **32**, 471 (1936).
17. Reed, D.A., and Ehrlich, G., *Surface Science*, **102**, 588 (1981).
18. Adams, D.L., *Surface Science*, **42**, 12 (1974).
19. Goymour, G.G., and King, D.A., *J. Chem. Soc. Faraday I*, **69**, 736 (1973).
20. Bridge, M.E., and Lambert, R.M., *Proc. Roy. Soc. (London)*, **A370**, 545 (1980); *Surface Science*, **94**, 469 (1980).
21. Sundaresan, S., Paper presented at the AIChE Annual Meeting, Los Angeles, 1982.
22. Kohler, V., and Wassmuth, M.W., *Surface Science*, **117**, 668 (1982); **126**, 448 (1983).

23. Astegger, St., and Bechtold, E., *Surface Science*, **122**, 491 (1982).
24. Bonzel, H.P., and Ku, R., *J. Chem. Phys.*, **59**, 1641 (1973).
25. Schmidt, M., and Siebert, W., *Comprehensive Inorganic Chemistry: The Chemistry of S*, Pergamon, Long Island City, NY (1975).
26. Engel, T., and Ertl, G., *Adv. Catal.*, **28**, 2 (1979).
27. Kaza, K.R., and Sundaresan, S., Paper presented at International Chemical Reaction Engineering Conference, Poona, India, January 1984.
28. Takoudis, C.G., Schmidt, L.D., and Aris, R., *Chem. Eng. Sci.*, **37**, 69 (1982).
29. Sales, B.C., Turner, J.E., and Maple, M.B., *Surface Sci.*, **114**, 381 (1982).
30. Jensen, K.F., and Ray, W.H., *Chem. Eng. Sci.*, **35**, 2439 (1980); **37**, 1387 (1982).